

Article

Structure-guided Design and Development of Potent and Selective Dual Bromodomain 4 (BRD4)/Polo-like Kinase 1 (PLK1) Inhibitors

Shuai Liu, Hailemichael O Yosief, Lingling Dai, He Huang, Gagan Dhawan, Xiaofeng Zhang, Alex M. Muthengi, Justin Roberts, Dennis L. Buckley, Jennifer A. Perry, Lei Wu, James E. Bradner, Jun Qi, and Wei Zhang

J. Med. Chem., **Just Accepted Manuscript** • DOI: 10.1021/acs.jmedchem.8b00765 • Publication Date (Web): 20 Aug 2018

Downloaded from <http://pubs.acs.org> on August 20, 2018

Just Accepted

“Just Accepted” manuscripts have been peer-reviewed and accepted for publication. They are posted online prior to technical editing, formatting for publication and author proofing. The American Chemical Society provides “Just Accepted” as a service to the research community to expedite the dissemination of scientific material as soon as possible after acceptance. “Just Accepted” manuscripts appear in full in PDF format accompanied by an HTML abstract. “Just Accepted” manuscripts have been fully peer reviewed, but should not be considered the official version of record. They are citable by the Digital Object Identifier (DOI®). “Just Accepted” is an optional service offered to authors. Therefore, the “Just Accepted” Web site may not include all articles that will be published in the journal. After a manuscript is technically edited and formatted, it will be removed from the “Just Accepted” Web site and published as an ASAP article. Note that technical editing may introduce minor changes to the manuscript text and/or graphics which could affect content, and all legal disclaimers and ethical guidelines that apply to the journal pertain. ACS cannot be held responsible for errors or consequences arising from the use of information contained in these “Just Accepted” manuscripts.



Structure-guided Design and Development of Potent and Selective Dual Bromodomain 4 (BRD4)/Polo-like Kinase 1 (PLK1) Inhibitors

Shuai Liu,^a Hailemichael O. Yosief,^a Lingling Dai,^{b,c} He Huang,^d Gagan Dhawan,^{a,e} Xiaofeng Zhang,^a Alex M. Muthengi,^a Justin Roberts,^f Dennis L. Buckley,^f Jennifer A. Perry,^b Lei Wu,^b James E. Bradner,^{f,g*} Jun Qi,^{b,h*} Wei Zhang^{a,*}

^a Department of Chemistry, University of Massachusetts-Boston, Boston, MA 02125, USA

^b Department of Cancer Biology, Dana-Farber Cancer Institute, Boston, MA 02215, USA

^c Phase I Clinical Trial Center & Department of Clinical Pharmacology, Xiangya Hospital, Central South University, Changsha, Hunan, 410008, P.R. China

^d Department of Chemistry, Stony Brook University, Stony Brook, New York 11794-3400

^e Department of Biomedical Science, Acharya Narendra Dev College, University of Delhi, New Delhi-110019, India

^f Department of Medical Oncology, Dana-Farber Cancer Institute, Boston, MA 02215, USA

^g Novartis Institute of Biomedical Research Institute, Cambridge, MA 02139, USA

^h Department of Medicine, Harvard Medical School, Boston, MA 02115, USA

Abstract: The simultaneous inhibition of polo-like kinase 1 (PLK1) and BRD4 bromodomain by a single molecule could lead to the development of an effective therapeutic strategy for a variety of diseases in which PLK1 and BRD4 are implicated. Compound **23** has been found to be a potent dual kinase-bromodomain inhibitor (BRD4-BD1 IC₅₀ = 28 nM, PLK1 IC₅₀ = 40 nM). Compound **6** was found to be the most selective PLK1 inhibitor over BRD4 in our series (BRD4-BD1 IC₅₀ = 2,579 nM,

1 PLK1 IC_{50} = 9.9 nM). Molecular docking studies with **23** and BRD4-BD1/PLK1 as well as with **6**
2
3 corroborates the biochemical assay results.
4

5
6 **Keywords:** Epigenetics, Bromodomains, BET, BRD4, PLK1 Kinases, BI-2536, Anti-cancer, Structure
7
8 guided design
9

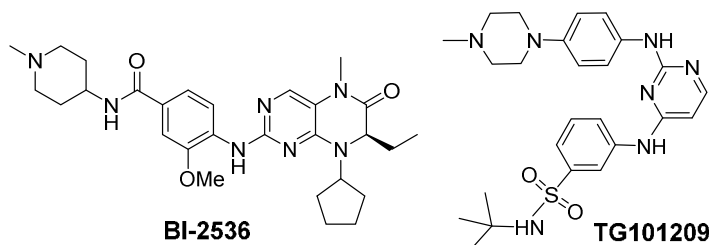
10 11 12 INTRODUCTION 13

14
15 The bromodomain and extra-terminal domain (BET) family of proteins is essential for
16 recognizing acetylated lysines (KAc) on chromatin and has emerged as a potential therapeutic target
17 for the treatment of cancer, inflammation and viral infectious diseases.¹⁻⁸ BET proteins, including
18 BRD2, BRD3, BRD4 and BRDT, are characterized by dual bromodomains (BD1 and BD2) that bind
19 to KAc on histones to facilitate the recruitment and stabilization of protein complexes, which plays an
20 active role in gene expression.⁹⁻¹³ With the development of the first small molecule inhibitor of BET
21 bromodomains, (+)-JQ1, we were able to demonstrate that binding to BRD4 displaces BRD4 from
22 chromatin and interrupts the biological function of the protein.^{3,14} Since our initial reports, several
23 potent and selective BET inhibitors with different chemotypes have been reported to possess similar
24 binding affinities, selectivity profiles and cellular activity as (+)-JQ1.¹⁵⁻¹⁹ More importantly, more than
25 twelve BET bromodomain inhibitors have progressed into clinical trials, including a derivative of
26 JQ1,²⁰ for the treatment of hematologic malignancies, solid tumors and cardiovascular disease.²¹ With
27 multiple cancer studies demonstrating the development of resistance to single agents, including BET
28 inhibitors, strategies for combination therapies are being intently pursued.²²⁻²⁴
29
30
31
32
33
34
35
36
37
38
39
40
41
42
43
44
45
46
47

48 Recent reports highlight that inhibition of polo-like kinase 1 (PLK1), a crucial cell-cycle
49 regulator, synergizes with BET inhibition in multiple cancer types, including prostate cancer and acute
50 myeloid leukemia (AML).^{25,26} While combinatorial inhibition of PLK1 and BET bromodomains with
51 two molecules is appears to be synergistic,²⁶ achieving this with a single agent may increase potency
52
53
54
55
56
57
58
59
60

1 for two disease-relevant targets/pathways while decreasing toxicity. The concept has recently been
2 demonstrated with dual PI3K-BRD4 inhibitors have recently been reported to block expression of the
3
4 MYC oncogene, while markedly inhibiting cancer cell growth and metastasis in hepatocellular
5
6 carcinoma and neuroblastoma *in vivo*.^{27,28} The recent discovery that multiple kinase inhibitors,
7
8 including PLK1 inhibitor, BI-2536, and the janus kinase 2 (JAK2) inhibitor, TG101209 (Fig. 1)
9
10 exhibit moderate to excellent inhibitory activity against BET family of proteins opens up the
11
12 possibility of creating polypharmacological compounds that target both kinases and BET proteins
13
14 equivalently.^{7,23,29-32}
15
16
17
18
19

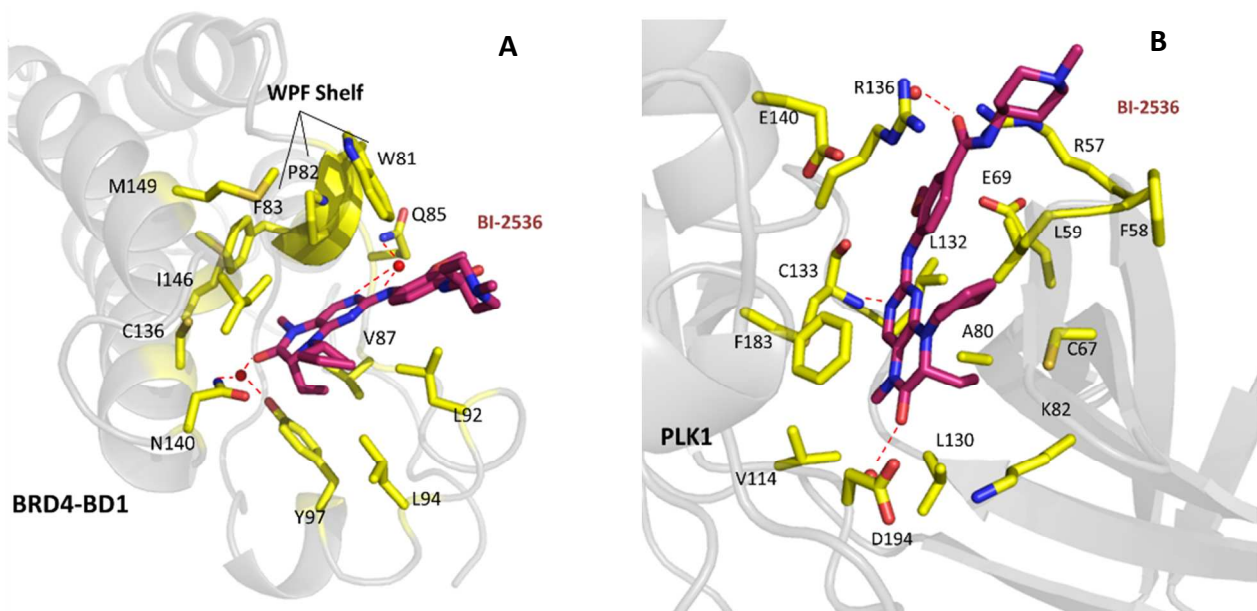
20
21 In this study, we utilized the scaffold of BI-2536 to develop inhibitors with varied inhibitory
22
23 activities against BRD4 and PLK1 in order to perform structure-activity relationship (SAR) studies, as
24
25 well as understand the effect of inhibiting both proteins (PLK1 and BRD4) with a single agent in
26
27 cancer, as both the BET family of proteins and PLK1 are intently pursued targets for the treatment of
28
29 cancer.
30



41
42 **Figure 1.** Kinase inhibitors with nanomolar inhibitory activity against BRD4
43

44
45 First, we inspected the binding modes of BI-2536 with BRD4-BD1 and PLK1, respectively,
46
47 through co-crystallization studies (Fig. 2). In the binding complex of BI-2536 with BRD4-BD1, the
48
49 methylated amide functions as an acetylated lysine mimic, where the carbonyl oxygen of the
50
51 dihydropteridinone ring forms a water-mediated hydrogen bond with conserved acetyl lysine
52
53 recognition motif, asparagine (N140) in the binding pocket. The methyl group is orientated into a
54
55
56
57
58
59
60

1 hydrophobic sub-pocket formed by F83, I146, and C136. The NH group on the aniline and one of the
2 pyrimidine nitrogen atoms interact with the Q85 backbone amide through an intermediary water
3 molecule. The ethyl group that branches off the asymmetric dihydropteridinone carbon atom is
4 projected into a small hydrophobic sub-pocket formed by V87, L92, L94, Y97, while the cyclopentyl
5 moiety and the *N*-methylpiperidine are both solvent exposed.^{29,30}
6
7
8
9
10
11
12
13
14
15



35 **Figure 2.** Crystal structure of BI-2536 (dark red) bound to A) BRD4-BD1 (PDB ID: 4O74) and B)
36 PLK1 (PDB ID: 2RKU). The protein residues in contact with ligand showed in yellow sticks; hydrogen
37 bonding showed in red dashed lines; the rest residues near binding pocket showed in gray.
38
39
40
41

42 Based on structural information from the co-crystals, we envisioned several strategies to improve
43 the BRD4-BD1 binding affinity while reducing the PLK1 inhibition to achieve balanced dual
44 PLK1/BRD4-BD1 inhibition (Fig. 3). First, we hypothesize that the replacement of the amide methyl
45 group at Site 1 with a slightly larger ethyl or isopropyl might enhance binding affinity to BRD4-BD1.
46 Second, to decrease affinity for PLK1, the elaboration of the 3-methoxy group on the aromatic ring
47 (Site 2) with a bulkier group might modulate binding affinity. This methyl ether group is involved in
48
49
50
51
52
53
54
55
56
57
58
59
60

critical hydrogen bonds with the PLK1 active site (Fig. 2B). The interruption of this interaction is expected to reduce the PLK1 binding affinity of BI-2536 but render its activity to BRD4-BD1 unchanged. Third, modification on ethyl group might have more impact on PLK1 activity as the pocket in PLK1 is narrower compared to the binding pocket in BRD4-BD1. In the end, we will modify the solvent exposed sites (Sites 4 and 5) to fully investigate the effect of each group on the binding affinity of the parent compound toward BRD4-BD1 and PLK1 based on the chemistry we established previously developing fluorescently-tagged kinase inhibitors.³¹ Thus, we conducted a medicinal chemistry campaign around the BI-2536 core to develop small molecules with fine-tuned activities against PLK1 and BET bromodomains.

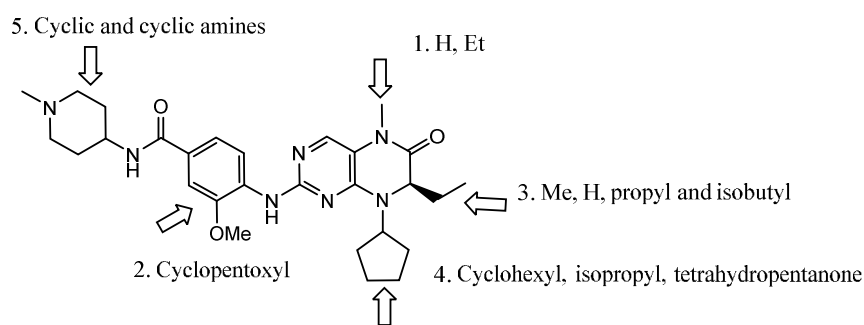
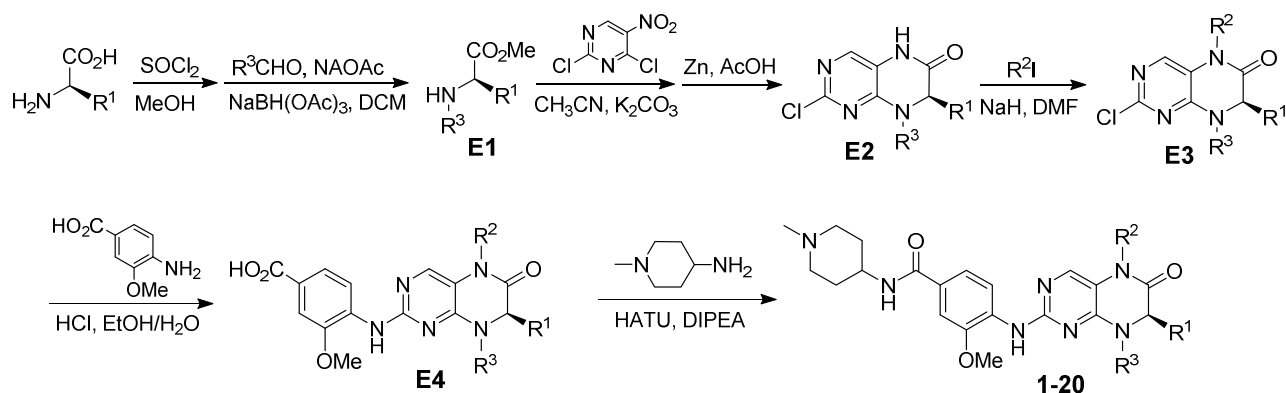


Figure 3. Available modification sites on BI-2536

RESULTS AND DISCUSSION

Utilizing the structural information from the co-crystal structures of BI-2535 with BRD4-BD1 and PLK1, a series of BI-2536 analogs were synthesized using the general synthetic route shown in Scheme 1. In brief, amino acids with varying alkyl side chains (different R¹ group) were esterified with thionyl chloride in MeOH followed by alkylation using reductive amination with cyclic or acyclic ketones. The resulting secondary amine derivative **E1** underwent a regioselective nucleophilic aromatic substitution reaction with 2,6-dichloro-5-nitropyrimidine to produce tertiary anilines. The

nitro group was reduced using zinc dust in hot acetic acid generating the dihydropteridinone ring in **E2**. Methylation of the amide produced the scaffold **E3**, which was used in a nucleophilic substitution reaction with the aminobenzoic acid derivative and led to the formation of intermediate **E4** with an acid motif, which was coupled with different amines to produce the final BI-2536 analogs. As planned in Figure 3, the resulting analogs include derivatives with different substituent groups on the amide bond (Site 1); different ethers at Site 2 with cyclic or acyclic motifs; varying substituent groups, such as hydrogen, methyl, propyl and isobutyl on Site 3; and the solvent exposed Site 4 or 5. All compounds in this focused library were then screened for their inhibitory activity against BRD4-BD1 and BRDT-BD1 using AlphaScreen assay technology to obtain IC₅₀ values (all IC₅₀ values are for BD1 of all of the bromodomains tested unless otherwise noted).³²



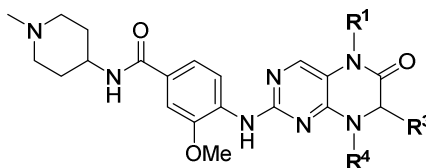
Scheme 1. Synthesis of BI-2536 analogs **1-20**

The modification of the cyclopentyl moiety at Site 4 with different cyclic and acyclic groups, cyclohexyl (compound **1**) and isopropyl (compound **2**), created compounds with nanomolar inhibitory activity against BRD4 (Table 1). These analogs, however, were less potent than the parent compound BI-2536, indicating that the cyclopentyl group is crucial for the potent inhibitory activity against BRD4. These compounds, however, maintained low nanomolar inhibitory activity against PLK1 suggesting that modification on Site 4 is tolerated for PLK1 binding. On the other hand, unmethylated

amide derivatives of compounds **1** and **2** (compound **3** and **4**, respectively) resulted in more than 1000-fold decrease in binding affinity for BRD4. Interestingly, the inhibitors with unmethylated amide, compounds **3** and **4**, displayed more than 250-fold selectivity for PLK1 over BRD4, indicating the importance of the methylated amide as an *N*-acetylated lysine mimic for BRD4 binding. Thus, it is critical to have a methylated amide at Site 1 to serve as *N*-acetylated lysine mimic for bromodomain inhibition. Taken together, the replacement of cyclopentyl group at site 4 together with an unmethylated amide reduce the BRD4 activity of the inhibitors while maintaining PLK1 selectivity.

Next, we examined the modification of Site 3 with methyl (compound **5**), propyl (compound **6**), hydrogen (compound **7**) and isobutyl (compound **8**) substituents. The analogue with methyl substitution at the asymmetric dihydropteridinone carbon atom, compound **5**, exhibited good inhibitory activity against both BRD4 ($IC_{50} = 84$ nM) and PLK1 ($IC_{50} = 11$ nM). Selectivity profiling against 32 bromodomains (BROMOscan®) and 468 kinases (KINOMEscan®)³³ confirmed selective activity for the BET subfamily and PLK kinases (PLK1-3) at 1 μ M through profiling platform at DiscoverX. Specifically, 1 μ M compound **5** exhibited selective activity against BRD4-BD1 (12% of control) and PLK kinases (0.3-0.5% of control) (Sup Inf Fig. 1). No significant difference in binding activity was observed for the (*S*) and (*R*) isomers of the methyl substituent, which is similar to the observation made on the (*S*) and (*R*) isomers of BI-2536 by the Fletcher group.³² However, replacing the asymmetric ethyl group with bulky alkyl groups like propyl (compound **6**) and isobutyl (compound **8**) resulted in a significant decrease in binding affinity towards BRD4. While compound **6** displayed excellent inhibitory activity against PLK1, with more than 250-fold selectivity over BRD4, further increasing the size of Site 3 to isobutyl, or deleting the methyl group resulted in a reduction of PLK1 inhibitory activity.

Table 1. Structure Activity Relationships on BI-2536 Analogs



Compound	R ⁴	R ³	R ¹	IC ₅₀ (uM)		
				^a BRD4-BD1	^b PLK1	^a BRDT-BD1
BI-2536	Cp	(<i>R</i>)-Et	Me	0.205±0.008	0.004	ND
1	Cy	(<i>R</i>)-Et	Me	0.65±0.024	0.004	ND
2	<i>i</i> -Pr	(<i>R</i>)-Et	Me	0.186±0.013	0.004	ND
3	<i>i</i> -Pr	(<i>R</i>)-Et	H	>10	2.62	ND
4	Cy	(<i>R</i>)-Et	H	>10	0.0372	ND
5	Cp	(<i>R</i>)-Me	Me	0.084±0.006	0.0011	0.342±0.015
6	Cp	(<i>R</i>)-Pr	Me	2.579±0.180	0.0099	8.468±0.076
7	Cp	H	Me	6.633±0.530	0.0541	25.99±9.70
8	Cp	(<i>R</i>)- <i>i</i> Bu	Me	18.8±3.4	0.078	ND
9	Cp	(<i>S</i>)-Me	Me	0.107±0.002	0.0087	0.229±0.010
10	Cp	(<i>S</i>)-Et	Me	0.489±0.017	0.0325	3.513±0.351
11	Cy	(<i>R</i>)-Me	Me	0.31±0.01	0.0086	0.75±0.03
12	<i>i</i> -Pr	(<i>R</i>)-Me	Me	0.421±0.016	0.0252	0.978±0.043
13	tetrahydro(2 <i>H</i>)pyran	(<i>R</i>)- <i>i</i> Bu	Me	>50	0.322	>50
14	<i>i</i> -Pr	(<i>R</i>)- <i>i</i> Bu	Me	41.9	0.218	ND
(S)-JQ1				0.032±0.001	-	0.103±0.004

^aIC₅₀ values were measured by AlphaScreen™ binding assay and reported as the average of 3 replicates ± SE.

^bIC₅₀ values were measured using Adapta assay format (ThermoFisher Scientific)

1 With the improvement in BRD4 inhibitory activity with compound **5**, we further examined this
2
3 compound through the replacement of the cyclopentyl group with cyclohexyl (compound **11**),
4
5 tetrahydro-2H-pyran (compound **13**) and isopropyl (compound **12**) groups. None of these substitutions
6
7 improved potency towards BRD4 above that seen for compound **5**, further indicating that substituting
8
9 the cyclopentyl moiety for the methyl group at the dihydropteridinone ring is optimal for BRD4
10
11 inhibition. On the other hand, the inhibitory activity of those analogs against PLK1 remained in the
12
13 low nanomolar range. Similarly replacing the cyclopentyl group of compound **8** with tetrahydro-2H-
14
15 pyran (compound **13**) and isopropyl (compound **14**) groups did not improve potency towards BRD4
16
17 but showed modest inhibitory activity against PLK1 suggesting that PLK1 is tolerant of substitutions
18
19 at the asymmetric carbon and anilide nitrogen (Table 1). Taken together, the adjustment of substituent
20
21 groups at the Site 3 tunes down BRD4 activity with little impact on PLK1 activity, leading us to
22
23 discover the most PLK1 selective inhibitor in the series, compound **6** (> 260 fold).
24
25
26
27
28

29 To increase the BRD4 selectivity of BI-2536 analogs, we utilized compound **5** to further explore
30
31 the SAR around the terminal amine (Site 5) and the methoxy group at Site 2 to investigate their impact
32
33 on potency and selectivity (Table 2, synthetic route shown in Scheme 2). Replacement of the terminal
34
35 cyclic amine (amino-piperidine, Site 5) with different alkyl and aromatic amines (compounds **15**, **16**,
36
37 **17**, **18**, **19** and **20**) did not grossly impact the potency and selectivity for BRD4, implying that the
38
39 various amine replacements are not engaged in any significant interaction with the amino acid residues
40
41 in the binding
42
43
44
45
46
47
48
49
50
51
52
53
54
55
56
57
58
59
60

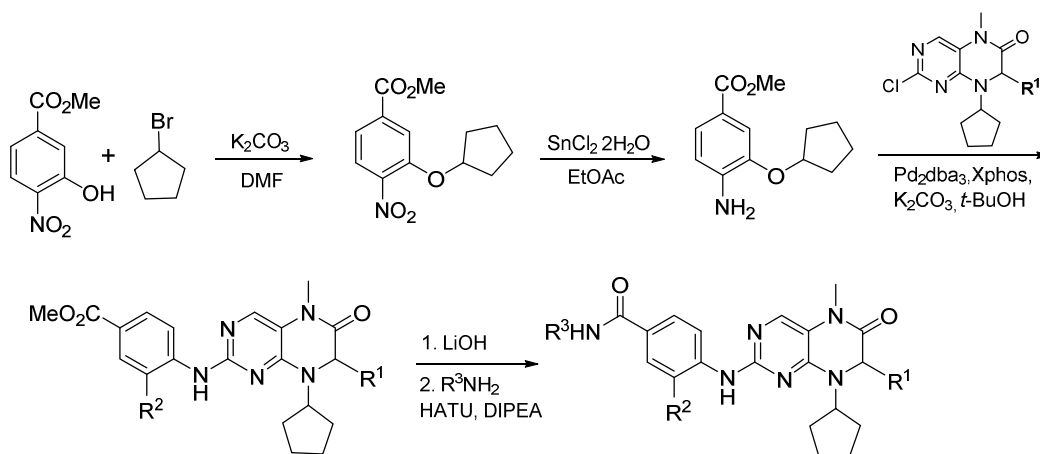
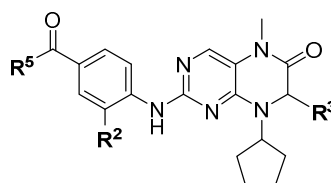
Scheme 2. Synthesis of compounds **21** and **23-25**

Table 2. Structure Activity

Relationship on Compound **5**

Analog



Compound	R ³	R ²	R ⁵	IC ₅₀ (uM)		
				^a BRD4-BD1	^b PLK1	^a BRDT-BD1
5	(R)-Me	OMe	4-amine, 1-methylpiperidine	0.084±0.006	0.0011	0.342±0.015
15	(R)-Me	OMe	hexamethylene amine	0.107±0.003	0.16	0.378±0.014
16	(R)-Me	OMe	aminomethylpyridine	0.095±0.002	0.0084	0.289±0.008
17	(R)-Me	OMe	phenylethylamine	0.183±0.009	0.027	0.558±0.015
18	(R)-Me	OMe	<i>N,N</i> -dimethylethylamine	0.104±0.050	0.021	0.392±0.013
19	(R)-Me	OMe	aminopiperidine	0.109±0.003	0.009	0.56±0.025
20	(R)-Me	OMe	piperidine	0.094±0.002	0.095	0.369±0.011
21	(S)-Me	O-Cp	4-amine, 1-methylpiperidine	0.059±0.001	0.127	0.245±0.009
22	(R)-Me	O-Cp	OMe	0.253±0.007	0.457	0.933±0.032
23	(R)-Me	O-Cp	4-amine, 1-methylpiperidine	0.028±0.001	0.04	0.102±0.002
24	(R)-Pr	O-Cp	4-amine, 1-methylpiperidine	0.596±0.014	0.047	1.951±0.080
25	H	O-Cp	4-amine, 1-methylpiperidine	0.69±0.018	-	3.543±0.198

^aIC₅₀ values were measured by AlphaScreen™ binding assay and reported as the average of 3 replicates ± SE.

^bIC₅₀ values were measured using Adapta assay format (ThermoFisher Scientific)

1 pocket of BRD4. On the other hand, the modification of methoxy moiety (Site 2) with a cyclopentoxyl
2 group improved potency toward bromodomains while reducing the potency against PLK1. These
3 substitutions created a molecule that has relatively balanced potency toward both PLK1 and BRD4
4 with less than 2-fold selectivity difference (Table 2). Notably, compound **23** exhibited improved
5 potency for BRD4 compared to our reference BET inhibitor, (+)-JQ1, but reduced activity against
6 PLK1 compared to BI-2536, making it one of the most potent BET bromodomain inhibitors with
7 reduced PLK1 inhibition in the series. This improvement can be overridden by introducing a larger
8 propyl group (compound **24**) at the Site 1. Also, the (*S*)-isomer of compound **23**, compound **21**,
9 retains good inhibitory activity against BRD4, but is less potent toward PLK1 suggesting that the
10 chirality change has more impact on PLK1 activity than BRD4 activity, which is consistent with the
11 SAR we established in the previous round. Finally, we examined the three compounds with the most
12 balanced BRD4 and PLK1 activity (compounds **5**, **6**, and **23**) in a human acute myeloid leukemia
13 (AML) cell line, MOLM13. In general, BRD4 bromodomain inhibition causes a G1 arrest in the cell
14 cycle as demonstrated by JQ1, while dual PLK1/BRD4 inhibitors, such as BI-2536, cause a G1/G2
15 arrest in the cell cycle. Twenty-four-hour treatment with compound **23** caused cell cycle arrest in the
16 G1/G2 stage of the cell cycle, suggesting that it is functionally inhibiting both BRD4 and PLK1 (Sup
17 Inf Fig. 2).

18 To gain a better understanding of the potency and predict the binding modes of our BI-2536
19 analogs, we utilized molecular modeling with PLK1 and BRD4-BD1 (Table 3). As described above,
20 compound **23** shows equivalent potency for both BRD4 and PLK1, while compound **6** demonstrates
21 the most selectivity for PLK1 over BRD4 in the series. To gain a better understanding of how
22 compound **23** interacts with BRD4, we further modeled the docking of **23** with BRD4-BD1. As shown
23 in Fig. 4B, all of the interactions between residues on BRD4 and BI-2536 are conserved when **23**
24 resides in the active site of BRD4. The conserved phenyl ring in the center of compound **23** develops
25
26
27
28
29
30
31
32
33
34
35
36
37
38
39
40
41
42
43
44
45
46
47
48
49
50
51
52
53
54
55
56
57
58
59
60

π - π stacking interactions with the aromatic rings in the WPF shelf (W81, P82, F83) of BRD4 as seen with the parental compound BI-2536. Furthermore, almost all of the original binding patterns established in our co-crystallography study of BI-2536 and BRD4 (Figure 2) are strengthened as indicated by the van der

Molecule	Docking score (Kcal/Mol)		IC ₅₀ (uM)		Ligand-receptor interactions (vdw energy < -4 kcal/mol)	
	BRD4	PLK1	BRD4	PLK1	BRD4	PLK1
23	-7.34	-8.46	0.028	0.0400	Pro82, Gln85, Val87, Ile146	Leu59, Cys133, Arg136, Phe183
6	-6.54	-8.68	2.579	0.0099	Trp81, Pro82, Gln85, Val87, Leu92	Leu59, Arg136, Phe183
8	-6.63	-7.62	18.80	0.0780	Gln85, Val87, Asp88	Gly63, Asp194
5	-6.50	-8.23	0.084	0.0011	Val87, Asp88, Ile146	Leu59, Arg136, Phe183
BI-2536	-7.02	-8.60	0.025	0.00083	Leu92, Ile146	Arg57, Leu59, Arg136, Phe183

Table 3. Docking results of some BI-2536 analogs on BRD4 and PLK1 (Details in SI)

Waals (vdw) interaction energy decomposition, where stronger interactions formed with P82, Q85, V87, C136, N140, I146 and compound **23** (Fig. 4A). Although the L92, L94 and Y97 hydrophobic sub-pocket of BRD4 is moved further from the dihydropteridinone, the deep pocket formed by F83, I146 and M149 made closer contact with the newly embedded cyclopentane to compensate or even gain back the hydrophobic interaction loss (Fig. 4B). Overall, the docking analysis of compound **23** with BRD4 is consistent with the binding affinity defined in our biochemical assays.

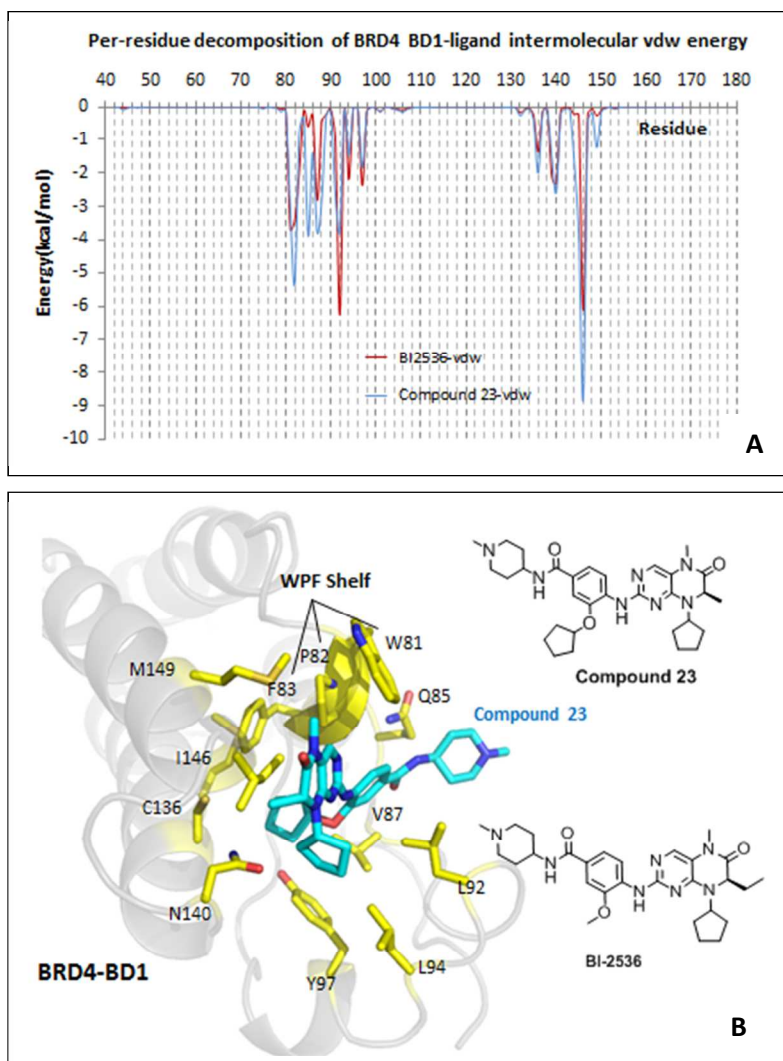


Figure 4. A. Comparison of the per-residue decomposition of two BRD4-BD1-ligand **23** in blue, BI-2536 in red intermolecular vdw interactions as a function of receptor sequence. B. Docking of **23** (cyan) with BRD4-BD1 (PDBID: 4O74), protein residues in contact with ligand shown in yellow sticks, the rest in gray.

In modeling the docking between compound **23** and PLK1, we found that the C133 backbone amide nitrogen of PLK1 conserves its hydrogen bonding to the nitrogen of dihydropteridinone in **23**, as indicated by unchanged dips at residue C133 from the vdw energy decomposition. The π - π stacking interaction between F83 and the dihydropteridinone in **23** is also conserved (Fig. 5A). The resulting docking pose of **23** with PLK1 retains similar interactions as BI-2536 with PLK1 (Fig. 5B). In addition,

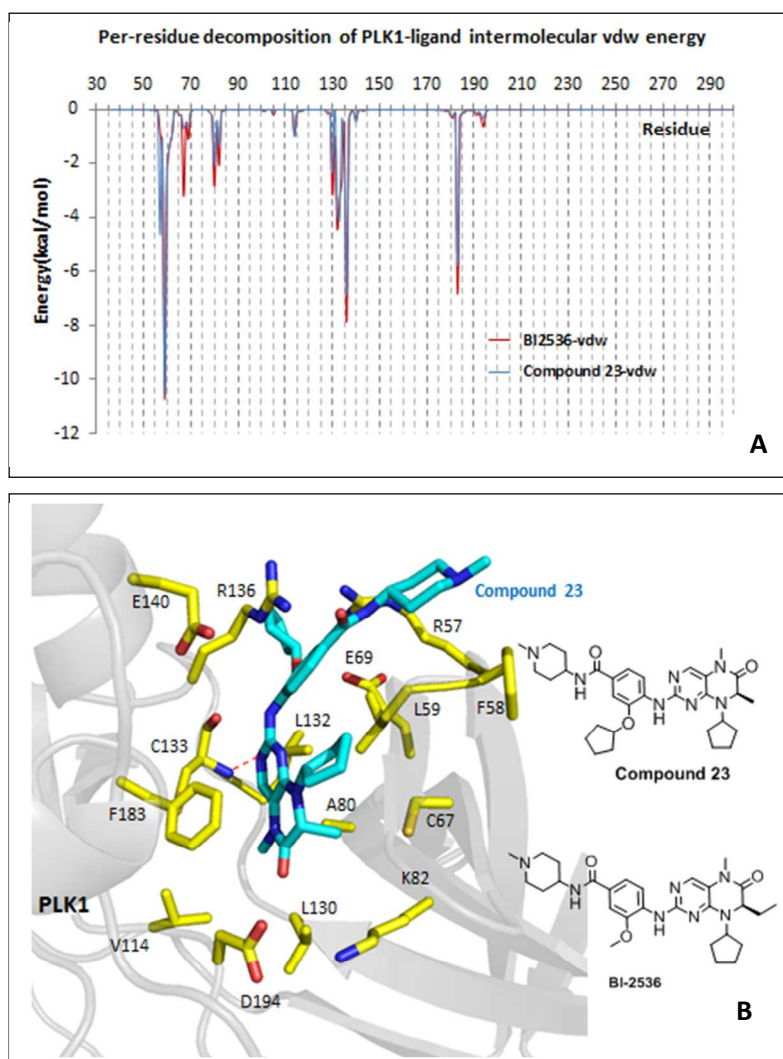


Figure 5. A. Comparison of the per-residue decomposition of two PLK1-ligand **23** in blue, BI-2536 in red intermolecular vdw interactions as a function of receptor sequence. B. Docking of **23** (cyan) in PLK1 (PDBID: 2RKU), protein residues in contact with ligand shown in yellow sticks, the rest in gray, hydrogen bonding in red dashed line. the methyl group in **23**, which replaced the original ethyl group in BI-2536, does not reduce interactions with A80 and K82 significantly. However, a notable difference upon the substitution of cyclopentane for the methyl group in **23**, is that the cyclopentane extends deeper into the hydrophobic sub-pocket between R57, F58 and L59 and creates additional interaction with R136, E140 that could further stabilize the overall binding.

Molecular modeling of compound **6** with BRD4-BD1 demonstrates that its docking pose demonstrates drastic variation from the co-crystal structure of BRD4-BD1 bound to BI-2536. When

1 BI-2536 binds to BRD4-BD1, the dihydropteridinone and cyclopentane rings rest in between the WPF
2 shelf (W81, P82, F83) and the BC loop (particularly N140 through bridging water) of BRD4-BD1,
3
4 with the ethyl group of BI-2536 pointing away to make additional contacts with V87, L92, L94 and
5
6
7
8 Y97 (sharing the bridging water with N140) (Figs. 6A & 6B). With BI-2536, Q85 interacts with the
9
10 inhibitor through water-mediated hydrogen bonding effect. However, the longer alkyl chain of
11
12 compound **6** breaks this interaction due to steric clashes with L94 and Y97 (Fig. 6C). Therefore,
13
14 compound **6** has to adapt a novel orientation in the BRD4-BD1 active site, which demonstrates much
15
16 weakened interactions by a striking positive vdw energy contribution from Y97. Although the phenyl
17
18 ring of compound **6** shifts into the pocket thereby enhancing binding with the WPF shelf, it still cannot
19
20 overcome the repulsive effect of the positive vdw effect. We believe that these adjustments contributed
21
22 significantly toward the reduced activity of **6** against BRD4-BD1.
23
24
25
26
27
28
29
30
31
32
33
34
35
36
37
38
39
40
41
42
43
44
45
46
47
48
49
50
51
52
53
54
55
56
57
58
59
60

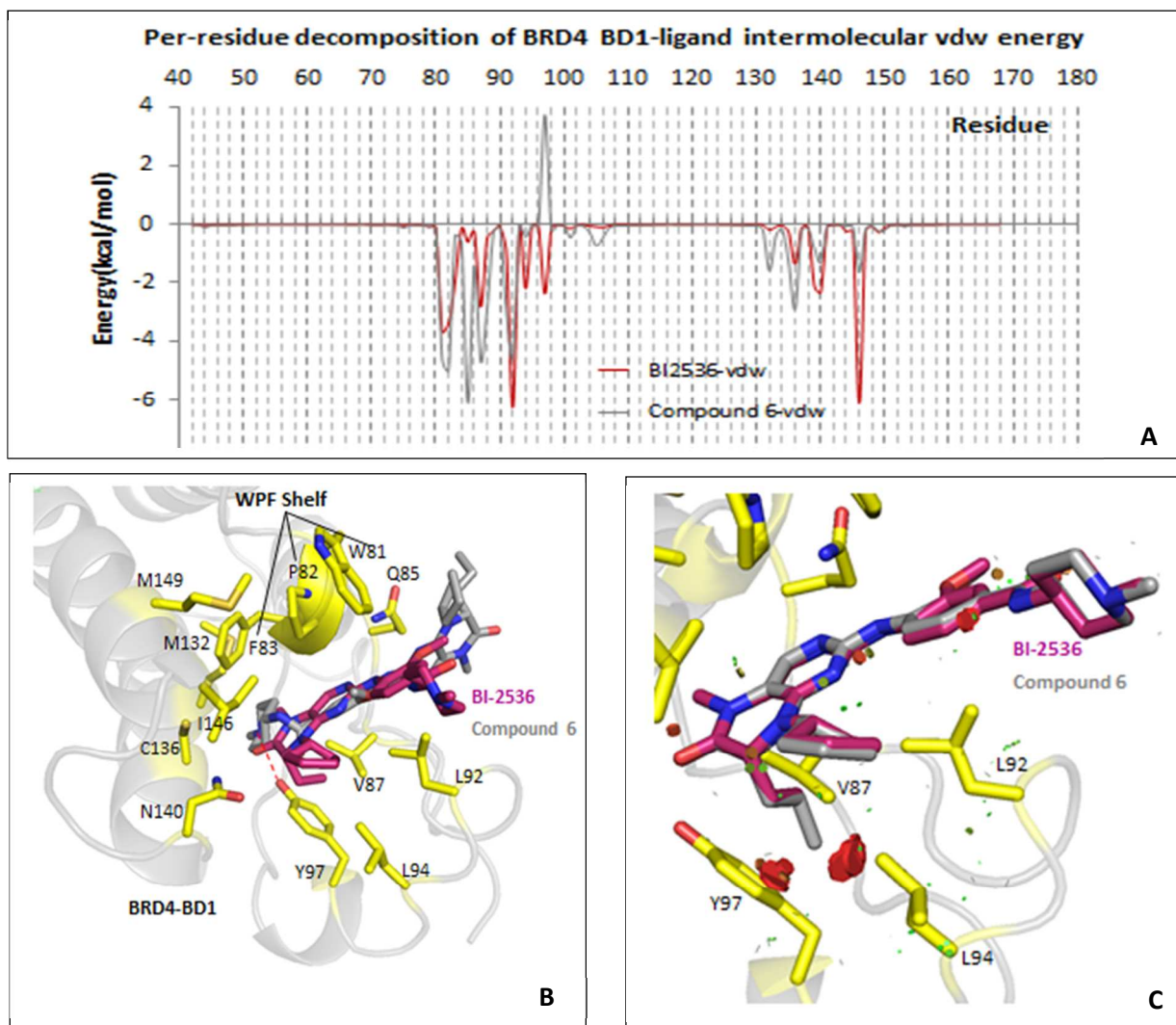


Figure 6. A. Comparison of the per-residue decomposition of two BRD4-BD1-ligand **6** in gray, BI-2536 in dark red intermolecular vdw interactions as a function of receptor sequence. B. Docking of **6** (gray) in BRD4 (1) (PDBID: 4O74), protein residues in contact with ligand shown in yellow sticks, the rest in gray). C. Steric clashes caused by the propyl group if **6** docked to BRD4(1) in the same pose as BI-2536 does (bumps shown in red dices).

Alternatively, the molecular docking of compound **6** with PLK1 shows great similarity with BI-2536 co-crystallized with PLK1. The residue C133 conserves as hydrogen bonding receptor to the nitrogen in the dihydropteridinone in **6**, and the π - π stacking interaction between F83 and the same aromatic ring (Figs. 7A & 7B). Furthermore, the propyl group in **6**, which replaced the original ethyl group in BI-2536 at Site 3, does not reduce interactions with A80 and K82 much. The docking pose suggests that the carbonyl oxygen moved away from the active site, but may form hydrogen bonds

with either R136, R57 or crystal water, as was observed in the BI-2536-PLK1 complex structure, to reduce the entropy penalty when the new complex is forming. Again, the molecular docking analysis is in agreement with the binding affinity assays that illustrate a potent interaction between PLK1 and **6**. The detailed ligand interaction diagrams (LID) are listed in Supplement Figs 3 & 4.

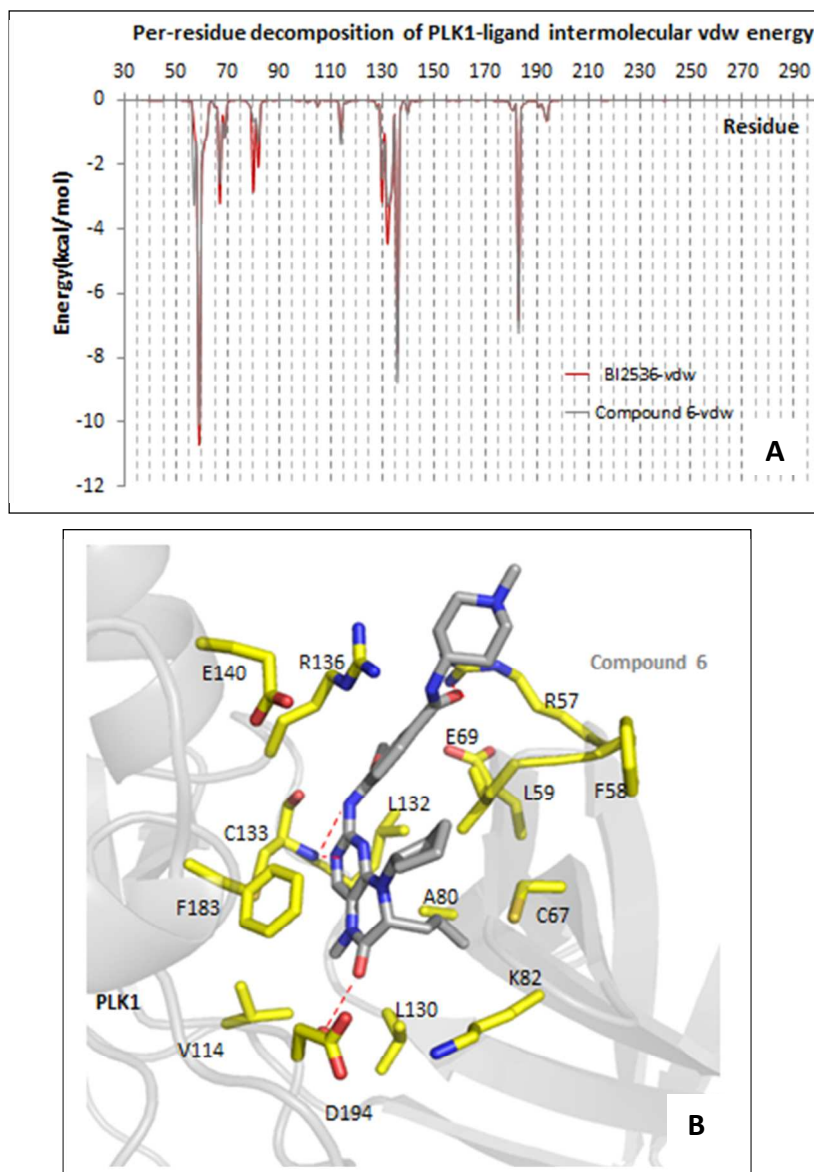


Figure 7. A. Comparison of the per-residue decomposition of two PLK1-ligand **6** in gray, BI-2536 in dark red intermolecular vdw interactions as a function of receptor sequence. B. Docking of **6** (gray) in PLK1 (PDBID: 2RKU), protein residues in contact with ligand shown in yellow sticks, the rest in gray, hydrogen bonding in red dashed line.

CONCLUSION

Our focused SAR study of the dual kinase-bromodomain inhibitor BI-2536 has led to the identification of potent, balanced inhibitors of BRD4 and PLK1, as well as a more PLK1 selective inhibitor. Through these studies, we determined the requirements for both PLK1 and BET protein binding. We determined that the methylated amide and the cyclopentyl group of the BI-2536 scaffold is important for maintaining bromodomain binding activity but less important for PLK1 inhibitory activity. Moreover, substituting the asymmetric ethyl moiety at the dihydropteridine ring with a methyl group improved the inhibitory activity of resulting compounds against both BRD4 and PLK1, as seen with compound **5**. Installing bulky alkyl groups at the asymmetric carbon resulted in inhibitors with potent and selective PLK1 activity but largely limited BRD4 activity, as seen with compound **6**. Further modification on the methoxy group of compound **5** led to the identification of compound **23**, a compound with increased potency for BRD4 with much reduced PLK1 activity. Our molecular docking studies suggested possible binding orientations with BRD4-BD1 and PLK1 and the binding energies were in agreement with the observed SAR established through our medicinal chemistry exercise.

In summary, we have demonstrated that fine-tuning the selectivity for inhibitors demonstrating polypharmacology can be achieved through structural guidance. We initiated an SAR campaign of BI-2536 in order to alter the PLK1 and BRD4 potency/selectivity of the compound and confirmed our biochemical findings through molecular modeling. In this study, we discovered a set of compounds with balanced selectivity against BRD4 and PLK1 that will entitle us to further explore the biological outcome of dual BRD4/PLK1 inhibition. In particular, compound **23** is a well-balanced BRD4 and PLK1 dual inhibitor when assayed biochemically and in cells. **23** demonstrates increased potency for BRD4 and decreased potency for PLK1 as compared to the parent molecule BI-2536. We envision

1 that this set of molecules will generate sufficient PLK1 and BRD4 inhibition in order to study
2 simultaneous targeting of PLK1 and BRD4 in cancer.
3
4

5 6 **EXPERIMENTAL SECTION**

7
8 **General Synthetic Information:** All chemicals and solvents were purchased from commercial
9 suppliers and used as received. ^1H NMR (300 MHz) and ^{13}C NMR (75 MHz) spectra were recorded on
10 a Varian NMR spectrometer, and ^1H NMR (400 MHz) and ^{13}C NMR spectra (101 MHz) were
11 recorded on Agilent NMR spectrometers. LC-MS were performed on an Agilent 2100 LC with a 6130
12 quadrupole MS spectrometers. Accurate mass measurements were performed on a Fusion Lumos
13 Orbitrap mass spectrometer (Thermo Fisher Scientific) at a mass resolution setting of 500000
14 immediately after calibration or under lock mass calibration using solvent ions. A C_{18} column (5.0 μm ,
15 6.0 x 50 mm) was used for separation. The mobile phases were MeOH and H_2O both containing
16 0.05% $\text{CF}_3\text{CO}_2\text{H}$. A linear gradient from 25:75 (v/v) MeOH/ H_2O to 100% MeOH over 7.0 min at a
17 flow rate of 0.7 mL/min was used as a mobile phase. UV detections were conducted at 210 nm, 254
18 nm and 365 nm. Low resolution mass spectra were recorded by APCI (atmospheric pressure chemical
19 ionization) unless otherwise specified. Flash chromatography separation was performed on
20 YAMAZEN AI-580 system with Agela silica gel (12 or 20 g, 230-400 mesh) cartridges. Final
21 products were purified on Angela HP-100 preparative-LC system with a Venusil PrepG- C_{18} column
22 (10 μm , 120 Å, 21.2 mm x 250 mm). All biologically evaluated compounds were found to be >95%
23 pure as determined by NMR and LCMS.
24
25
26
27
28
29
30
31
32
33
34
35
36
37
38
39
40
41
42
43
44

45 **Synthesis of BI-2536 analogs.** The synthesis of compounds **1-20** shown in Tables 1 and 2 was
46 carried out following the reported procedures (Scheme 1).³⁴ The synthesis of analogs of compound **5**
47 including compounds **21**, **23-25** listed in Table 2 was performed following the route shown in Scheme
48 2. Bromocyclopentane (1.3 equiv) was added slowly to a stirred suspension of potassium carbonate
49 (1.5 equiv) in DMF containing methyl- 3-hydroxy-4-nitrobenzoate (1 equiv) at 65 °C for 4 h, then the
50
51
52
53
54
55
56
57
58
59
60

product was treated by SnCl₂·2H₂O in EtOAc at 50 °C overnight. A mixture of Ar-Cl (1 equiv), X-Phos (28 mol %), Pd₂(dba)₃ (7 mol %), methyl 4-amino-3-(cyclopentyloxy)benzoate (1.3 equiv), and K₂CO₃ (5 equiv) in *t*-BuOH was heated at 100 °C in a sealed-tube for 8 h. The mixture was then diluted with EtOAc and washed three times with aqueous NaHCO₃. The organic layer was dried over anhydrous Na₂SO₄, filtered and condensed. The crude product was purified by preparative-LC system to get the final product.

(*R*)-4-((8-cyclopentyl-5,7-dimethyl-6-oxo-5,6,7,8-tetrahydropteridin-2-yl)amino)-3-methoxy-*N*-(1-methylpiperidin-4-yl)benzamide (Compound 5). ¹H NMR (300 MHz, CD₃OD) δ 8.41 (1H, d, *J* = 9.0 Hz), 7.72 (1H, s), 7.41 - 7.31 (3H, m), 4.50 - 4.45 (1H, m), 4.31 - 4.24 (1H, q, *J* = 6.7 Hz), 4.02 - 3.82 (6H, s, N-CH₃ and O-CH₃), 3.27 - 3.26 (6H, m), 3.22 (3H, s), 2.57 - 2.47 (6H, m), 2.06 - 1.86 (4H, m), 1.25 (3H, d, *J* = 6.6 Hz); ¹³C NMR (75 MHz, CD₃OD) δ 170.9, 166.6, 156.3, 153.0, 139.44, 138.7, 127.3, 121.2, 117.3, 117.3, 109.9, 59.5, 59.3, 56.4, 55.6, 55.02, 47.1, 44.9, 31.2, 30.5, 29.9, 28.5, 24.3, 23.8, 19.0; HRMS (ESI) *m/z*: (M+H)⁺ calcd for C₂₇H₃₇N₇O₃ 536.3349, found 508.3031 (M⁺+1).

(*R*)-4-((8-cyclopentyl-5-methyl-6-oxo-7-propyl-5,6,7,8-tetrahydropteridin-2-yl)amino)-3-methoxy-*N*-(1-methylpiperidin-4-yl)benzamide (Compound 6). ¹H NMR (400 MHz, CDCl₃) δ 8.54 (1H, d, *J* = 8.4 Hz), 7.68 (1H, s), 7.59 (1H, s), 7.51 (1H, s), 7.42 (1H, s), 7.42 (1H, d, *J* = 1.8 Hz), 4.56 - 4.46 (1H, m), 4.24 (1H, dd, *J* = 8.0, 3.7 Hz), 3.97 (3H, s), 3.31 (3H, s), 2.86 - 2.84 (2H, m), 2.31 (3H, s), 2.25 - 2.10 (4H, m), 2.07 - 2.04 (4H, m), 1.81 - 1.71 (14H, m), 1.37 - 1.21 (4H, m), 0.87 (3H, t, *J* = 7.3 Hz); ¹³C NMR (101 MHz, CDCl₃) δ 163.9, 155.0, 152.1, 147.2, 137.9, 133.2, 126.2, 126.0, 118.8, 116.4, 115.8, 109.0, 58.8, 58.1, 54.4, 35.8, 32.4, 29.6, 29.1, 28.2, 23.5, 23.0, 17.8, 13.9; HRMS (ESI) *m/z*: (M+H)⁺ calcd for C₂₉H₄₁N₇O₃ 536.3349, found 536.3342 (M⁺+1).

(*R*)-4-((8-cyclopentyl-7-isobutyl-5-methyl-6-oxo-5,6,7,8-tetrahydropteridin-2-yl)amino)-3-methoxy-*N*-(1-methylpiperidin-4-yl)benzamide (Compound 8). ¹H NMR (300 MHz, CD₃OD) δ

8.40 (1H, d, $J = 9.0$ Hz), 7.74 (1H, s), 7.42 – 7.38 (3H, m), 4.21 – 4.17 (1H, m), 3.91 (3H, s), 3.87 – 3.83 (1H, m), 3.23 (3H, s), 2.91 – 2.88 (1H, m), 2.27 (3H, s), 2.21 – 2.13 (2H, m), 2.02 – 1.97 (2H, m), 1.92 – 1.83 (2H, m), 1.74 – 1.54 (8H, m), 1.41 – 1.36 (1H, m), 0.92 (3H, d, $J = 6.3$ Hz), 0.78 (3H, d, $J = 6.6$ Hz); ^{13}C NMR (75 MHz, CD_3OD) δ 169.1, 165.2, 156.2, 153.6, 148.4, 139.6, 134.0, 127.4, 121.2, 117.4, 117.3, 109.9, 59.6, 58.4, 56.4, 55.5, 45.8, 42.5, 32.0, 30.49, 30.4, 28.6, 25.7, 24.2, 23.9, 23.7, 21.7; HRMS (ESI) m/z : $(\text{M}+\text{H})^+$ calcd for $\text{C}_{30}\text{H}_{43}\text{N}_7\text{O}_3$ 550.3506, found 550.3501 ($\text{M}^+ + 1$).

(*R*)-4-((8-isopropyl-5,7-dimethyl-6-oxo-5,6,7,8-tetrahydropteridin-2-yl)amino)-3-methoxy-*N*-(1-methylpiperidin-4-yl)benzamide (Compound 12). ^1H NMR (300 MHz, CD_3OD) δ 8.42 (1H, d, $J = 9.3$ Hz), 7.69 (1H, s), 7.38 (3H, m), 3.99 – 3.90 (5H, m), 3.90 (3H, s), 2.72 – 2.65 (4H, m), 2.55 (3H, s), 1.86-1.76 (4H, m), 1.30 – 1.23 (9H, m); ^{13}C NMR (75 MHz, CD_3OD) δ 169.2, 166.4, 156.3, 152.4, 148.3, 139.5, 134.1, 127.1, 121.3, 117.2, 109.8, 56.4, 54.7, 53.6, 46.6, 44.4, 30.7, 28.5, 21.5, 19.9; HRMS (ESI) m/z : $(\text{M}+\text{H})^+$ calcd for $\text{C}_{25}\text{H}_{35}\text{N}_7\text{O}_3$ 482.2880, found 482.2884 ($\text{M}^+ + 1$).

(*R*)-4-((7-isobutyl-5-methyl-6-oxo-8-(tetrahydro-2H-pyran-4-yl)-5,6,7,8-tetrahydropteridin-2-yl)amino)-3-methoxy-*N*-(1-methylpiperidin-4-yl)benzamide (Compound 13). ^1H NMR (300 MHz, CD_3OD) δ 8.42 (1H, d, $J = 9.0$ Hz), 7.78 (1H, s), 7.45 – 7.42 (3H, m), 3.92 (3H, s), 3.56 – 3.53 (2H, m), 3.22 (3H, s), 3.03 – 2.99 (2H, m), 2.37 (3H, m), 1.96 – 1.92 (3H, m), 1.70 – 1.65 (4H, m), 1.55 – 1.38 (5H, m), 0.94 (3H, d, $J = 6.3$ Hz), 0.79 (3H, d, $J = 6.6$ Hz); ^{13}C NMR (75 MHz, CD_3OD) δ 171.5, 171.4, 170.9, 169.1, 164.86, 153.0, 150.0, 140.1, 127.5, 121.2, 117.4, 110.0, 68.6, 68.5, 57.3, 56.4, 55.3, 55.2, 45.4, 43.4, 32.6, 31.6, 28.7, 25.8, 23.9, 21.7; HRMS (ESI) m/z : $(\text{M}+\text{H})^+$ calcd for $\text{C}_{30}\text{H}_{43}\text{N}_7\text{O}_4$ 566.3455, found 566.3448 ($\text{M}^+ + 1$).

(*S*)-4-((8-cyclopentyl-5,7-dimethyl-6-oxo-5,6,7,8-tetrahydropteridin-2-yl)amino)-3-methoxy-*N*-(1-methylpiperidin-4-yl)benzamide (Compound 21). ^1H NMR (300 MHz, CD_3OD) δ 8.43 (1H, d, $J = 8.7$ Hz), 7.75 (1H, s), 7.43 – 7.41 (3H, m), 4.31 – 4.29 (1H, q, $J = 6.0$ Hz), 3.94 (3H, s), 3.24 (3H, s),

3.12-3.07 (3H, m), 2.90 - 2.87 (3H, m), 2.12 - 2.09 (3H, m), 1.91 - 1.89 (4H, m), 1.79 - 1.67 (6H, m),
1.26 (3H, d, $J = 6.9$ Hz); ^{13}C NMR (75 MHz, CD_3OD) δ 171.1, 169.1, 166.6, 156.2, 153.0, 148.3,
139.4, 134.0, 127.4, 121.2, 117.2, 109.9, 59.3, 56.4, 55.6, 55.4, 47.8, 45.7, 31.9, 30.5, 29.9, 28.5, 24.2,
23.8, 19.0; HRMS (ESI) m/z : $(\text{M}+\text{H})^+$ calcd for $\text{C}_{31}\text{H}_{43}\text{N}_7\text{O}_3$ 562.3506, found 562.3501 ($\text{M}^+ + 1$).

(*R*)-4-((8-cyclopentyl-5,7-dimethyl-6-oxo-5,6,7,8-tetrahydropteridin-2-yl)amino)-3-(cyclopentyloxy)-*N*-(1-methylpiperidin-4-yl)benzamide (Compound 23). ^1H NMR (400 MHz, CDCl_3) δ 8.53 (1H, d, $J = 8.0$ Hz), 7.71 (1H, s), 7.60 (1H, s), 7.41 (1H, d, $J = 1.9$ Hz), 4.62 - 4.51 (1H, m), 4.32 - 4.30 (1H, m), 4.14 - 4.06 (1H, m), 3.97(3H, s), 3.31 (3H, s), 2.83 - 2.81 (3H, m), 2.29 (3H, s), 2.20 - 2.10 (3H, m), 2.08 - 1.93 (4H, m), 1.32 (3H, d, $J = 6.8$ Hz); ^{13}C NMR (101 MHz, CDCl_3) δ 166.6, 165.0, 155.2, 151.8, 147.2, 138.3, 133.1, 126.6, 118.8, 116.3, 116.0, 109.1, 57.6, 55.9, 54.4, 46.2, 32.5, 30.0, 29.5, 28.3, 23.7, 23.2, 19.0. HRMS (ESI) m/z : $(\text{M}+\text{H})^+$ calcd for $\text{C}_{31}\text{H}_{43}\text{N}_7\text{O}_3$ 562.3506, found 562.3508 ($\text{M}^+ + 1$).

(*R*)-4-((8-cyclopentyl-5-methyl-6-oxo-7-propyl-5,6,7,8-tetrahydropteridin-2-yl)amino)-3-(cyclopentyloxy)-*N*-(1-methylpiperidin-4-yl)benzamide (Compound 24). ^1H NMR (300 MHz, CD_3OD) δ 8.44 (1H, d, $J = 8.1$ Hz), 7.72 (1H, s), 7.42 - 7.39 (3H, m), 4.39 - 4.34 (1H, m), 4.27- 4.24 (1H, m), 3.85 - 3.80 (1H, m), 3.25 (3H, s), 2.86 - 2.60 (2H, m), 2.26 (3H, s), 2.16 - 2.09 (3H, m), 2.01 - 1.80 (14H, m), 1.76 - 1.59 (8H, m), 1.26 - 1.17 (2H, m), 0.83 (3H, t, $J = 7.2$ Hz); ^{13}C NMR (75 MHz, CD_3OD) δ 169.12, 165.4, 156.0, 153.4, 146.5, 139.0, 134.8, 127.3, 120.8, 117.2, 112.4, 81.8, 60.67 60.5, 55.6, 49.7, 46.0, 36.8, 33.6, 32.2, 30.2, 29.9, 28.4, 24.8, 24.4, 24.2, 18.7, 14.0; HRMS (ESI) m/z : $(\text{M}+\text{H})^+$ calcd for $\text{C}_{33}\text{H}_{47}\text{N}_7\text{O}_3$ 590.3819, found 590.3815 ($\text{M}^+ + 1$).

4-((8-cyclopentyl-5-methyl-6-oxo-5,6,7,8-tetrahydropteridin-2-yl)amino)-3-(cyclopentyloxy)-*N*-(1-methylpiperidin-4-yl)benzamide (Compound 25). ^1H NMR (300 MHz, CD_3OD) δ 8.43 (1H, d, $J = 8.4$ Hz), 7.64 (1H, s), 7.42 - 7.39 (3H, m), 4.06 (3H, s), 3.28 - 3.25 (4H, m), 3.23 (3H, s), 3.02 - 2.97

(3H, m), 2.37 (3H, s), 2.30 – 2.26 (3H, m), 1.98 – 1.93 (7H, m), 1.74 – 1.68 (9H, m); ^{13}C NMR (75 MHz, CD_3OD) δ 169.1, 163.5, 156.1, 153.1, 146.4, 138.5, 134.8, 127.1, 120.8, 117.0, 116.8, 112.3, 81.8, 56.9, 55.37, 47.6, 45.9, 45.5, 33.6, 31.7, 28.0, 27.9, 24.8, 24.8; HRMS (ESI) m/z : $(\text{M}+\text{H})^+$ calcd for $\text{C}_{30}\text{H}_{41}\text{N}_7\text{O}_3$ 548.3350, found 548.3346 ($\text{M}^+ + 1$).

Molecular Docking Software: For protein preparation: UCSF Chimera Dock Prep tool,³⁵ UCSF DOCK6.³⁶ For compound structures and charge assignment method: ChemDraw 15.0, Chem3D 14.0, GAFF, AM1-BCC. For docking and energy decomposition analysis: UCSF DOCK6 suite. Dock poses, visualization and illustration: UCSF Chimera ViewDock, PyMOL.

Compounds and protein preparation: The synthesized compounds were built in ChemDraw, and then their Cartesian coordinates' construction and energy minimization using MM2 force field^{37,38} were generated in Chem3D. The crystal structures of BI-2536 binding with BRD4-BD1 (PDBID: 4O74) and PLK1 (PDBID: 2RKU) were downloaded from Protein Data Bank (PDB). Protein targets were prepared using Chimera DockPrep tool, in which AMBER force field ff14SB³⁹ was employed to provide accurate descriptions for proteins. GAFF⁴⁰ and AM1-BCC⁴¹ were used to generate parameters and assign charges for all inhibitor molecules.

Docking and energy decomposition analysis: DOCK6 suite was used for docking compounds to their protein targets. Flexible ligand docking was performed under the guidance of the anchor-and-grow algorithm. Dock Score was used as the criterion for ranking the binding poses. We visually examined the top 10 ranked poses, and the highest ranked poses are reported in Table 3. In the case of PLK1 and BRD4-BD1, DOCK6 successfully sampled and top-scored the BI-2536 docking poses to reproduce the corresponding crystal binding poses with $\text{rmsd} < 2 \text{ \AA}$. DOCK Score is composed of Van der Waals (vdw) and electrostatic interactions. The vdw composition of Dock score was further decomposed onto every residue of its binder protein by using DOCK write_footprint function, which generates both the vdw and electrostatic parts. Only the vdw composition was noticeably diversified

1 and thus referred to represent the contribution of the protein target per residue in protein-ligand
2 interaction energy profiles as shown in Figures 4-7.
3
4

5
6 **Specific favorable and unfavorable interactions recognition:** As listed in Table 3, the specific
7 residual information of the protein receptors interacting with BI-2536 analogs was recognized by
8 referring to vdw energy and by visualization of binding poses. A threshold of < -4 kcal/mol in
9 decomposed vdw energy was used to include the first shell of residues around the molecules (see also
10 Sup Inf Fig S-3). The positive peak observed in per-residue decomposition of BRD4-DB1 compound
11 **6**, Figure 6A, was ascribed to the steric clashes of residue Y97, L94 with the propyl group on **6**. The
12 disc was scripted in PyMOL software to show vdw overlaps or steric clashing (See also Sup Inf Fig S-
13 4).
14
15
16
17
18
19
20
21
22
23

24 **BRD4-BD1 and BRDT-BD1 activity assays:** Compound potency was assessed by relative IC_{50}
25 potency determined by an AlphaScreen biotin-JQ1 competition assay as reported previously by our
26 group.⁴² All reagents were diluted in 50 mM HEPES, 150 mM NaCl, 0.1% w/v BSA, 0.01% w/v
27 Tween20, pH 7.5 and allowed to equilibrate to room temperature prior to the addition to plates. After
28 addition of Alpha beads to master solutions, all subsequent steps were performed in low light
29 conditions. A 2x solution of components with final concentrations of BRD at 40 nM, Ni-coated
30 Acceptor Bead at 25 $\mu\text{g/mL}$, and 20 nM biotin-JQ1 was added in 10 μL to 384-well plates (AlphaPlate
31 - 384, PerkinElmer, USA). After a 1 min 1000 rpm spin-down, 100 nL of compounds in DMSO from
32 stock plates were added by pin transfer using a Janus Workstation (PerkinElmer, USA). The 2x, 10 μL
33 streptavidin-coated donor beads (25 $\mu\text{g/ml}$) were added to the previous solution. Following this
34 addition, the plates were sealed with foil to block light exposure and to prevent evaporation. The plates
35 were spun down again at 1000 rpm for 1 min. Next, the plates were incubated at room temperature
36 with the plate reader (for temperature equilibration) for 1 h prior to reading the assay. Signal is stable
37
38
39
40
41
42
43
44
45
46
47
48
49
50
51
52
53
54
55
56
57
58
59
60

1 for up to 3 h after donor bead addition. AlphaScreen measurements were performed on an Envision
2
3
4 2104 (PerkinElmer, USA) utilizing the manufacturer's protocol.

5
6 **PLK1 activity assay:** The enzymatic activities against PLK1 were tested in Z-Lyte assays with
7
8 ATP concentration of K_M for each kinase per manufacturer's protocol (Thermo Fisher).
9

10 All the compounds were tested in parallel with cross-linker assay to rule out the assay
11
12 binder/interrupter.
13

14
15 **Selectivity profiling:** Compound **5** was assayed at 1 μ M in DiscoverX's BROMOscan®
16
17 (*bromoMAX*SM) and KINOMEscan® (*scanMAX*SM) assay platforms. The results for single
18
19 concentration binding interactions for compound **5** are reported as % of control (DMSO).
20
21

22 **Cell cycle study:** MOLM13 cells were treated with 1 μ M of JQ1, BI2536, TAE684, compound **5**,
23
24 compound **6** or compound **23** for 24 h. Cells were subsequently harvested and stained with propidium
25
26 iodide (Calbiochem), followed by measurement of propidium iodide-mediated fluorescence with a
27
28 Guava H6T (Millipore Sigma).
29
30

31 32 33 ASSOCIATED CONTENT

34 35 36 Supporting Information

37
38
39 The supporting information is available free of charge on the [ACS Publications](#) website at DOI: *****
40
41

42
43 BROMOscan and KINOMEscan data for compound 5 (CSV)
44

45
46 Molecular-formula strings (CSV)
47
48

49 50 Accession Codes

51
52 PDB codes are the following: 4O74 for BI2536: BRD4-BD1; 2RKU for PLK1-BI2536
53
54

55 56 AUTHOR INFORMATION

Corresponding Authors

*E-mail:

james.bradner@novartis.com. Tel.: +1 (617-871-8000. Fax: +1(617)-582-7370

jun_qi@dfci.harvard.edu. Tel.: +1 (617) 632-6629. Fax: +1(617) 582-7370

wei2.zhang@umb.edu. Tel.: +1 (617) 287-6147. Fax: +1 (617) 287-6030.

ORCID

James E. Bradner: 0000-0002-2718-4415

Jun Qi: 0000-0002-1461-3356

Wei Zhang: 0000-0002-6097-2763

Author Contributions

All authors have given approval to the final version of the manuscript.

Notes

The authors declare no competing financial interest.

ACKNOWLEDGMENTS

This work was partially supported by National Institutes of Health U54 grant CA156732 (JEB and WZ); U54 grant (HD093540-01 for JQ); P01 grant (CA066996 for JQ). We thank Jason Evans and Dennis Zeh for performing HRMS analysis of some synthetic compounds.

ABBREVIATIONS USED

1 BET, bromodomain and extra-terminal domain; BRD4, bromodomain 4; PLK1, polo-like kinase 1;
2
3 AML, acute myeloid leukemia; JAK2, janus kinase 2; SAR, structure-activity relationship; LID,
4
5 ligand interaction diagrams
6
7
8
9
10
11
12

13 REFERENCES

- 14
15
16
17
18 (1) Wang, C. Y.; Filippakopoulos, P. Beating the odds: BETs in disease. *Trends Biochem. Sci.*
19 **2015**, *40*, 468 – 479.
20
21 (2) Boehm, D.; Calvanese, V.; Dar, R. D.; Xing, S.; Schroeder, S.; Martins, L.; Aull, K.; Li, P. C.;
22 Planelles, V.; Bradner, J. E.; Zhou, M. M.; Siliciano, R. F.; Weinberger, L.; Verdin, E.; Ott, M. BET
23 bromodomain-targeting compounds reactivate HIV from latency via a Tat-independent
24 mechanism. *Cell Cycle (Georgetown, Tex.)* **2013**, *12*, 452 - 462.
25
26 (3) Delmore, J. E.; Issa, G. C.; Lemieux, M. E.; Rahl, P. B.; Shi, J.; Jacobs, H. M.; Kastiris, E.;
27 Gilpatrick, T.; Paranal, R. M.; Qi, J.; Chesi, M.; Schinzel, A. C.; McKeown, M. R.; Heffernan, T. P.;
28 Vakoc, C. R.; Bergsagel, P. L.; Ghobrial, I. M.; Richardson, P. G.; Young, R. A.; Hahn, W. C.; Anderson,
29 K. C.; Kung, A. L.; Bradner, J. E.; Mitsiades, C. S. BET bromodomain inhibition as a therapeutic
30 strategy to target c-Myc. *Cell* **2011**, *146*, 904 - 917.
31
32 (4) Bandukwala, H. S.; Gagnon, J.; Togher, S.; Greenbaum, J. A.; Lamperti, E. D.; Parr, N. J.;
33 Molesworth, A. M.; Smithers, N.; Lee, K.; Witherington, J.; Tough, D. F.; Prinjha, R. K.; Peters, B.;
34 Rao, A. Selective inhibition of CD4+ T-cell cytokine production and autoimmunity by BET protein
35 and c-Myc inhibitors. *Proc. Natl. Acad. Sci. U S A* **2012**, *109*, 14532 - 14537.
36
37 (5) Gallenkamp, D.; Gelato, K. A.; Haendler, B.; Weinmann, H. Bromodomains and their
38 pharmacological inhibitors. *ChemMedChem* **2014**, *9*, 438 - 464.
39
40 (6) Filippakopoulos, P.; Knapp, S. Targeting bromodomains: epigenetic readers of lysine
41 acetylation. *Nat. Rev. Drug Discov.* **2014**, *13*, 337 - 356.
42
43 (7) Prinjha, R. K.; Witherington, J.; Lee, K. Place your BETs: the therapeutic potential of
44 bromodomains. *Trends Pharmacol. Sci.* **012**, *33*, 146 - 153.
45
46
47
48
49
50
51
52
53
54
55
56
57
58
59
60

- 1 (8) Vidler, L. R.; Brown, N.; Knapp, S.; Hoelder, S. Druggability analysis and structural
2 classification of bromodomain acetyl-lysine binding Sites. *J. Med. Chem.* **2012**, *55*, 7346 -7359.
- 3 (9) Filippakopoulos, P.; Knapp, S. The bromodomain interaction module. *FEBS Lett.* **2012**,
4 *586*, 2692 - 2704.
- 5 (10) Hewings, D. S.; Rooney, T. P.; Jennings, L. E.; Hay, D. A.; Schofield, C. J.; Brennan, P. E.;
6 Knapp, S.; Conway, S. J. Progress in the development and application of small molecule inhibitors
7 of bromodomain–acetyl lysine interactions. *J. Med. Chem.* **2012**, *55*, 9393 - 9413.
- 8 (11) Chung, C. W. Small molecule bromodomain inhibitors: extending the druggable genome.
9 *Prog. Med. Chem.* **2012**, *51*, 1 - 55.
- 10 (12) Yang, Z.; Yik, J. H.; Chen, R.; He, N.; Jang, M. K.; Ozato, K.; Zhou, Q. Recruitment of P-TEFb
11 for stimulation of transcriptional elongation by the bromodomain protein Brd4. *Mol Cell* **2005**,
12 *19*, 535 - 545.
- 13 (13) Jang, M. K.; Mochizuki, K.; Zhou, M.; Jeong, H. S.; Brady, J. N.; Ozato, K. The bromodomain
14 protein Brd4 is a positive regulatory component of P-TEFb and stimulates RNA polymerase II-
15 dependent transcription. *Mol Cell* **2005**, *19*, 523 - 534.
- 16 (14) Filippakopoulos, P.; Qi, J.; Picaud, S.; Shen, Y.; Smith, W. B.; Fedorov, O.; Morse, E. M.;
17 Keates, T.; Hickman, T. T.; Felletar, I.; Philpott, M.; Munro, S.; McKeown, M. R.; Wang, Y.; Christie,
18 A. L.; West, N.; Cameron, M. J.; Schwartz, B.; Heightman, T. D.; La Thangue, N.; French, C. A.; Wiest,
19 O.; Kung, A. L.; Knapp, S.; Bradner, J. E. Selective inhibition of BET bromodomains. *Nature* **2010**,
20 *468*, 1067 - 1073.
- 21 (15) Nicodeme, E.; Jeffrey, K. L.; Schaefer, U.; Beinke, S.; Dewell, S.; Chung, C. W.; Chandwani, R.;
22 Marazzi, I.; Wilson, P.; Coste, H.; White, J.; Kirilovsky, J.; Rice, C. M.; Lora, J. M.; Prinjha, R. K.; Lee,
23 K.; Tarakhovsky, A. Suppression of inflammation by a synthetic histone mimic. *Nature* **2010**, *468*,
24 1119 - 1123.
- 25 (16) Mirguet, O.; Lamotte, Y.; Donche, F.; Toum, J.; Gellibert, F.; Bouillot, A.; Gosmini, R.;
26 Nguyen, V. L.; Delannee, D.; Seal, J.; Blandel, F.; Boullay, A. B.; Boursier, E.; Martin, S.; Brusq, J. M.;
27 Krysa, G.; Riou, A.; Tellier, R.; Costaz, A.; Huet, P.; Dudit, Y.; Trottet, L.; Kirilovsky, J.; Nicodeme, E.
28 From ApoA1 upregulation to BET family bromodomain inhibition: Discovery of I-BET151.
29 *Bioorg. Med. Chem. Lett.* **2012**, *22*, 2963 - 2967.
- 30 (17) Fish, P. V.; Filippakopoulos, P.; Bish, G.; Brennan, P. E.; Bunnage, M. E.; Cook, A. S.; Federov,
31 O.; Gerstenberger, B. S.; Jones, H.; Knapp, S.; Marsden, B.; Nocka, K.; Owen, D. R.; Philpott, M.;
32
33
34
35
36
37
38
39
40
41
42
43
44
45
46
47
48
49
50
51
52
53
54
55
56
57
58
59
60

- 1 Picaud, S.; Primiano, M. J.; Ralph, M. J.; Sciammetta, N.; Trzupek, J. D. Identification of a chemical
2 probe for bromo and extra C-terminal bromodomain inhibition through optimization of a
3 fragment-derived hit. *J. Med. Chem.* **2012**, *55*, 9831 - 9837.
- 4
5
6 (18) Tanaka, M.; Roberts, J. M.; Qi, J.; Bradner, J. E. Inhibitors of emerging epigenetic targets for
7 cancer therapy: A patent review (2010–2014). *Pharm. Pat. Anal.* **2015**, *4*, 261 - 284.
- 8
9
10 (19) Garnier, J. M.; Sharp, P. P.; Burns, C. J. BET bromodomain inhibitors: a patent review.
11 *Expert Opin. Ter. Pat.* **2014**, *24*, 185 - 199.
- 12
13 (20) Sanchez, R.; Meslamani, J.; Zhou, M. M. The bromodomain: from epigenome reader to
14 druggable target. *Biochim. Biophys Acta* **2014**, *1839*, 676 - 685.
- 15
16
17 (21) Shortt, J.; Ott, C. J.; Johnstone, R. W.; Bradner, J. E. A chemical probe toolbox for dissecting
18 the cancer epigenome. *Nat. Rev. Cancer* **2017**, *17*, 160 - 183.
- 19
20
21 (22) Shu, S.; Lin, C. Y.; He, H. H.; Witwicki, R. M.; Tabassum, D. P.; Roberts, J. M.; Janiszewska, M.;
22 Huh, S. J.; Liang, Y.; Ryan, J.; Doherty, E.; Mohammed, H.; Guo, H.; Stover, D. G.; Ekram, M. B.;
23 Brown, J.; D'Santos, C.; Krop, I. E.; Dillon, D.; McKeown, M.; Ott, C.; Qi, J.; Ni, M.; Rao, P. K.; Duarte,
24 M.; Wu, S. Y.; Chiang, C. M.; Anders, L.; Young, R. A.; Winer, E.; Letai, A.; Barry, W. T.; Carroll, J. S.;
25 Long, H.; Brown, M.; Liu, X. S.; Meyer, C. A.; Bradner, J. E.; Polyak, K. Response and resistance to
26 BET bromodomain inhibitors in triple-negative breast cancer. *Nature* **2016**, *529*, 413 - 417.
- 27
28
29 (23) Gutteridge, R. E.; Ndiaye, M. A.; Liu, X.; Ahmad, N. PLK1 inhibitors in cancer therapy: From
30 laboratory to clinics. *Mol. Cancer. Ther.* **2016**, *15*, 1427 - 1435.
- 31
32
33 (24) Seton-Rogers, S. Epigenetics: Place your BETs. *Nat. Rev. Cancer* **2015**, *15*, 638.
- 34
35
36 (25) Mao, F.; Li, J.; Luo, Q.; Wang, R.; Kong, Y.; Carlock, C.; Liu, Z.; Elzey, B. D.; Liu, X. PLK1
37 inhibition enhances the efficacy of bet epigenetic reader blockade in castration-resistant
38 prostate cancer. *Mol. Cancer Ther.* **2018**, *17*, 1554 - 1565.
- 39
40
41 (26) Tontsch-Grunt, U.; Rudolph, D.; Waizenegger, I.; Baum, A.; Gerlach, D.; Engelhardt, H.;
42 Wurm, M.; Savarese, F.; Schweifer, N.; Kraut, N. Synergistic activity of BET inhibitor BI 894999
43 with PLK inhibitor volasertib in AML in vitro and in vivo. *Cancer Lett.* **2018**, *421*, 112 - 120.
- 44
45
46 (27) Andrews, F. H.; Singh, A. R.; Joshi, S.; Smith, C. A.; Morales, G. A.; Garlich, J. R.; Durden, D. L.;
47 Kutateladze, T. G. Dual-activity PI3K–BRD4 inhibitor for the orthogonal inhibition of MYC to
48 block tumor growth and metastasis. *Proc. Natl. Acad. Sci. U S A* **2017**, *114*, E1072 – E1080.
- 49
50
51 (28) Singh, A. R.; Joshi, S.; Burgoyne, A. M.; Sicklick, J. K.; Ikeda, S.; Kono, Y.; Garlich, J. R.;
52 Morales, G. A.; Durden, D. L. Single agent and synergistic activity of the “first-in-class” Dual
53
54
55
56
57
58
59
60

1 PI3K/BRD4 inhibitor SF1126 with sorafenib in hepatocellular carcinoma. *Mol. Cancer Ther.*
2 **2016**, *15*, 2553 - 2562.

3
4 (29) Ember, S. W.; Zhu, J. Y.; Olesen, S. H.; Martin, M. P.; Becker, A.; Berndt, N.; Georg, G. I.;
5 Schonbrunn, E. Acetyl-lysine binding site of bromodomain-containing protein 4(BRD4) interacts
6 with diverse kinase inhibitors. *ACS Chem. Biol.* **2014**, *9*, 1160 - 1171.

7
8 (30) Ciceri, P.; Muller, S.; O'Mahony, A. Dual kinase-bromodomain inhibitors for rationally
9 designed polypharmacology. *Nat. Chem. Biol.* **2014**, *10*, 305 - 312.

10
11 (31) Koblan, L. W.; Buckley, D. L.; Ott, C. J.; Fitzgerald, M. E.; Ember, S. W.; Zhu, J. Y.; Liu, S.;
12 Roberts, J. M.; Remillard, D.; Vittori, S.; Zhang, W.; Schonbrunn, E.; Bradner, J. E. Assessment of
13 bromodomain target engagement by a series of BI2536 analogues with miniaturized BET-BRET.
14 *ChemMedChem* **2016**, *11*, 2575 - 2581.

15
16 (32) Chen, L.; Yap, J. L.; Yoshioka, M.; Lanning, M. E.; Fountain, R. N.; Raje, M.; Scheenstra, J. A.;
17 Strovel, J. W.; Fletcher, S. BRD4 structure-activity relationships of dual PLK1 Kinase/BRD4
18 bromodomain inhibitor BI-2536. *ACS Med. Chem. Lett.* **2015**, *6*, 764 - 769.

19
20 (33) Fabian, M. A.; Biggs, W. H., 3rd; Treiber, D. K.; Atteridge, C. E.; Azimioara, M. D.; Benedetti,
21 M. G.; Carter, T. A.; Ciceri, P.; Edeen, P. T.; Floyd, M.; Ford, J. M.; Galvin, M.; Gerlach, J. L.; Grotzfeld,
22 R. M.; Herrgard, S.; Insko, D. E.; Insko, M. A.; Lai, A. G.; Lelias, J. M.; Mehta, S. A.; Milanov, Z. V.;
23 Velasco, A. M.; Wodicka, L. M.; Patel, H. K.; Zarrinkar, P. P.; Lockhart, D. J. A small molecule-kinase
24 interaction map for clinical kinase inhibitors. *Nat. Biotechnol.* **2005**, *23*, 329 - 336.

25
26 (34) Zhang, Z.; Kwiatkowski, N.; Zeng, H.; Lim, S. M.; Gray, N. S.; Zhang, W., Yang, P. L.
27 Leveraging kinase inhibitors to develop small molecule tools for imaging kinases by fluorescence
28 microscopy. *Mol. BioSyst.* **2012**, *8*, 2523 - 2526.

29
30 (35) Pettersen, E. F., Goddard, T. D., Huang, C. C.; Couch, G. S.; Greenblatt, D. M.; Meng, E. C.;
31 Ferrin, T. E. UCSF Chimera - A visualization system for exploratory research and analysis. *J.*
32 *Comput. Chem.* **2004**, *25*, 1605 - 1612.

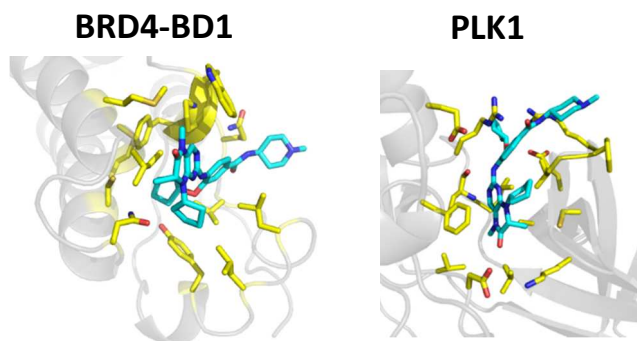
33
34 (36) Allen, W. J.; Balias, T. E.; Mukherjee, S.; Brozell, S. R.; Moustakas, D. T.; Lang, P. T.; Case, D.
35 A., Kuntz, I. D.; Rizzo, R. C. DOCK 6: Impact of new features and current docking performance. *J.*
36 *Comput. Chem.* **2015**, *36*, 1132 - 1156.

37
38 (37) Allinger, N. L. Conformational analysis. 130. MM2. A hydrocarbon force field utilizing V1
39 and V2 torsional terms. *J. Am. Chem. Soc.* **1977**, *99*, 8127 - 8134.

- 1 (38) Ponder, J. W.; Richards, F. M. An efficient newton-like method for molecular mechanics
2 energy minimization of large molecules. *J. Comput. Chem.* **1987**, *8*, 1016 - 1024.
3
4 (39) Maier, J. A.; Martinez, C.; Kasavajhala, K.; Wickstrom, L.; Hauser, K. E.; Simmerling, C.
5 ff14SB: Improving the accuracy of protein side chain and backbone parameters from FF99SB. *J.*
6 *Chem. Theory Comput.* **2015**, *11*, 3696 - 3713.
7
8 (40) Wang, J.; Wolf, R. M.; Caldwell, J. W.; Kollman, P. A.; Case, D. A. Development and testing of
9 a general amber force field. *J. Comput. Chem.* **2004**, *25*, 1157 - 1174.
10
11 (41) Jakalian, A.; Jack, D. B.; Bayly, C. I. Fast, efficient generation of high-quality atomic charges.
12 AM1 - BCC model: II. Parameterization and validation. *J. Comput. Chem.* **2002**, *23*, 1623 - 1641.
13
14 (42) McKeown, M. R.; Shaw, D. L.; Fu, H.; Liu, S.; Xu, X.; Marineau, J. J.; Huang, Y.; Zhang, X.;
15 Buckley, D. L.; Kadam, A.; Zhang, Z.; Blacklow, S. C.; Qi, J.; Zhang, W.; Bradner, J. E. Biased
16 multicomponent reactions to develop novel bromodomain inhibitors. *J. Med. Chem.* **2014**, *57*,
17 9019 - 9027.
18
19
20
21
22
23
24
25
26
27
28
29
30
31
32
33
34
35
36
37
38
39
40
41
42
43
44
45
46
47
48
49
50
51
52
53
54
55
56
57
58
59
60

1
2
3
4
5
6
7
8
9
10
11
12
13
14
15
16
17
18
19
20
21
22
23
24
25
26
27
28
29
30
31
32
33
34
35
36
37
38
39
40
41
42
43
44
45
46
47
48
49
50
51
52
53
54
55
56
57
58
59
60

Table of Contents graphic



Dual inhibitor: IC₅₀ BRD4-BD1 28 nM, PLK1 40 nM